

Infrared Optical Properties of Quasi-1D Topological Insulators: Bi_4Br_4 and Bi_4I_4

Quasi-1D Topological Quantum Materials Workshop • 6 January 2023

Spenser Talkington and Fan Zhang

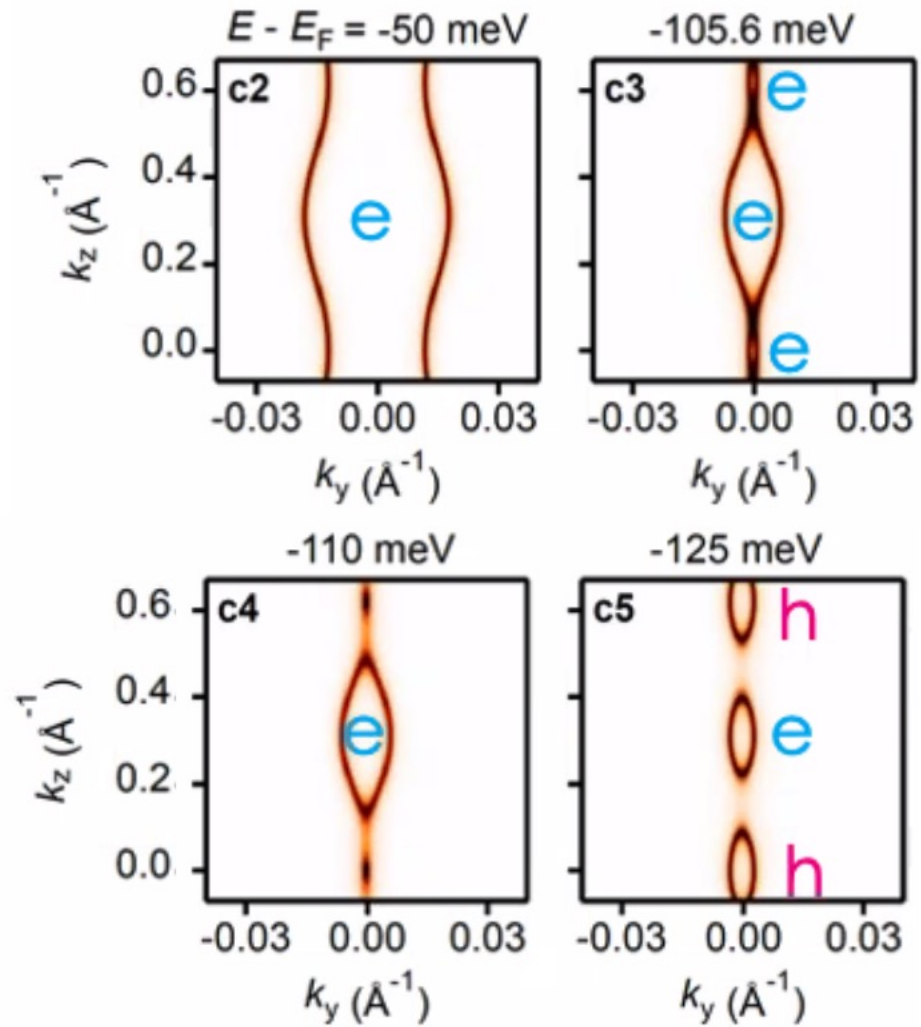
University of Pennsylvania and UT Dallas

Why Quasi-1D Materials?

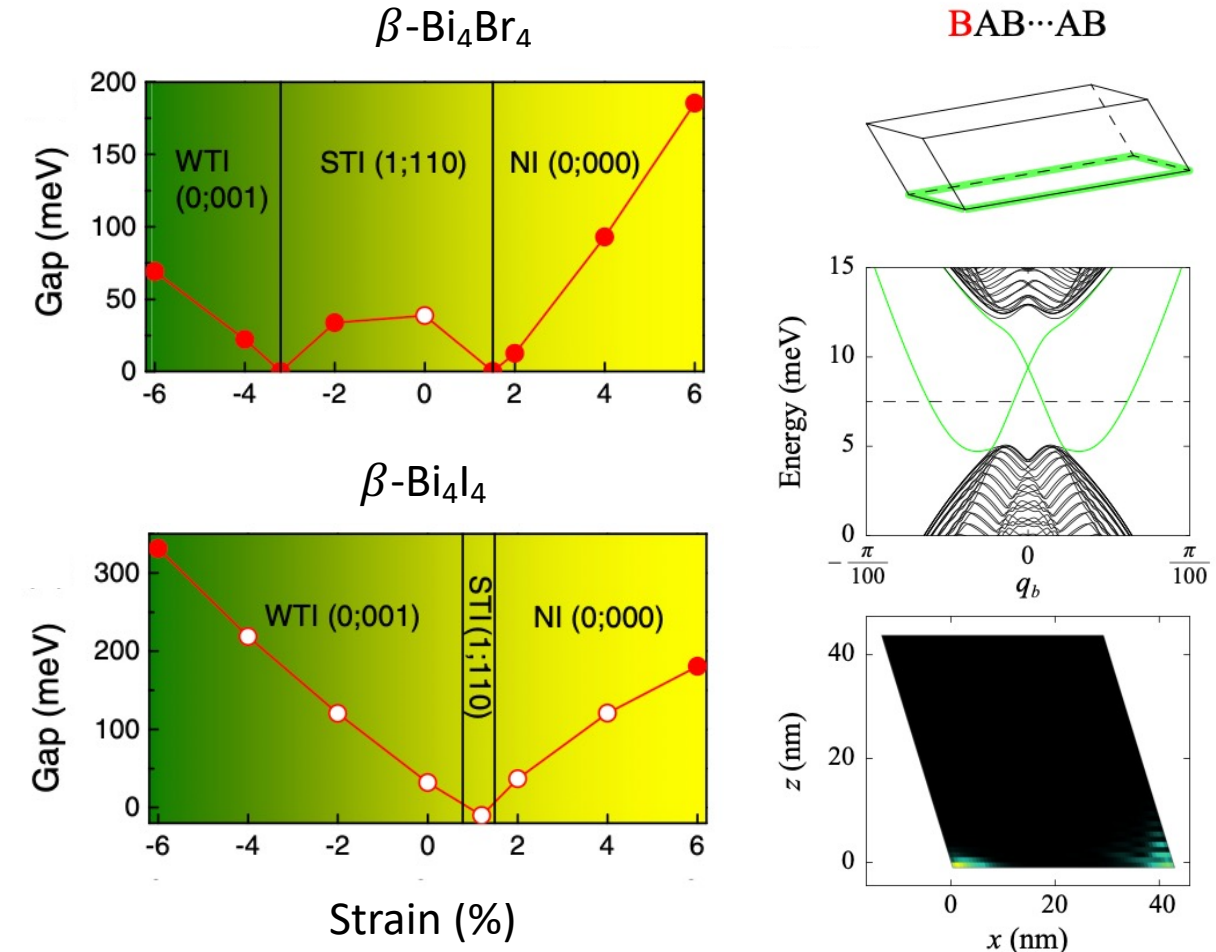
1/27

- We want to realize exotic states
- Weak TIs^{1,2}
 - Even numbers of Dirac cones on some surfaces
 - First realized in $\beta\text{-Bi}_4\text{I}_4$
- HOTIs^{3,4}
 - Edge state in $\alpha\text{-Bi}_4\text{Br}_4$ and $\alpha\text{-Bi}_4\text{I}_4$
- Luttinger liquids and exciton condensates

1. C.C. Liu, et al. PRL **116**, 066801 (2016)
2. R. Noguchi, et al. Nature **566**, 518 (2019)
3. C. Yoon, et al. arXiv 2005.14710 (2020)
4. J. Huang, et al. PRX **11**, 031042 (2021)



- How to realize a weak TI?
 - Stack weakly coupled QSH layers
 - D.F. Mross, et al. PRL **116**, 036803 (2016)
 - Quasi-1D material
 - C.C. Liu, et al. PRL **116**, 066801 (2016)
- Higher order TIs
 - F. Zhang, et al. PRL **110**, 046404 (2013)
 - W. A. Benalcazar, et al. Science **357**, 61 (2017)
 - C. Yoon, et al. arXiv 2005.14710 (2020)



Van der Waals Materials

3/27

- Direction-dependent bond strength leads to natural cleavage planes
- Good cleavage planes makes for easy access to surface and edge states
- Many materials are stacked 2D layers
- Relatively few in stacks of 1D chains
 - Bi_4X_4 , TaSe_3 , TaTe_4 , Nb_2Se_4 , NbCl_4 , MoI_3

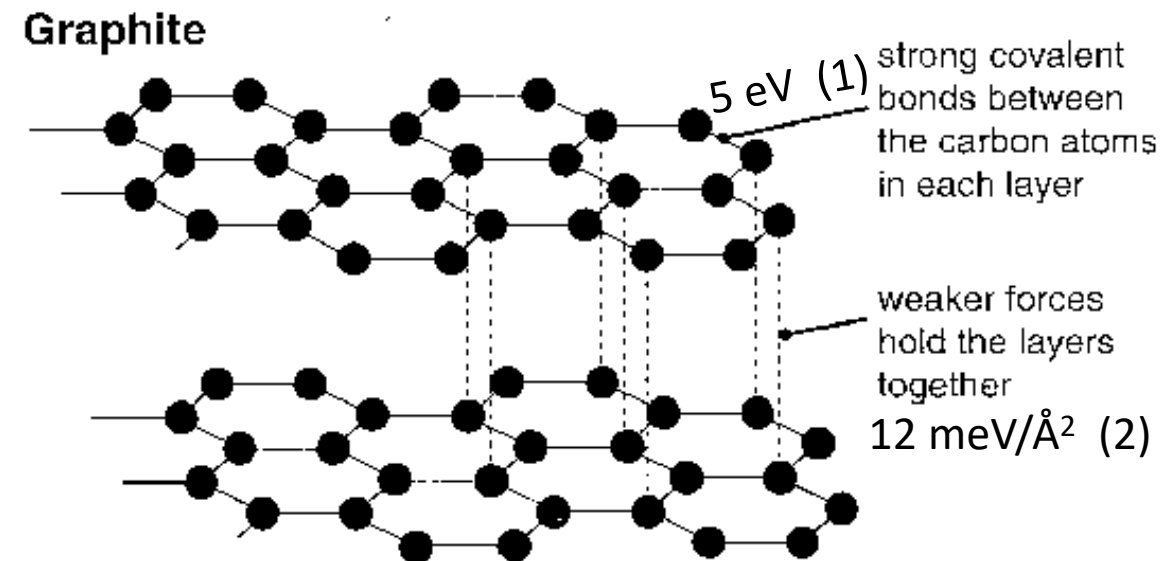


Image from J. Clark, Chemistry Libretexts, 14.4 (2021). CC BY-NC-SA 3.0.

1. D. Brenner, et al. *JPCM* **14** 783 (2002)
2. Z. Liu, et al. *PRB* **85**, 205418 (2012)

Structure of Quasi-1D Materials: Bi_4X_4

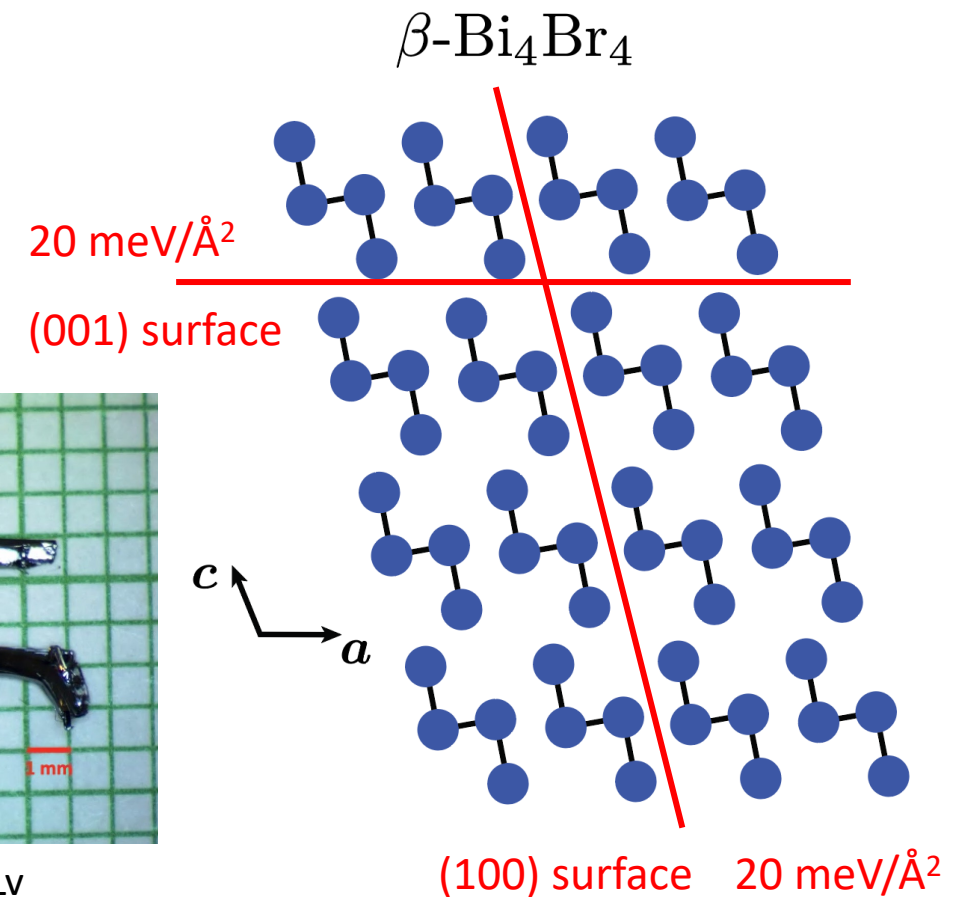
4/27

- Bi_4Br_4 and Bi_4I_4 are 1D chains that align to form 3D materials^{1,2,3}
- Two natural cleavage planes
 - (001) surface: trivial insulator¹
 - (100) surface: weak/strong TI¹

1. C.C. Liu, et al. PRL **116**, 066801 (2016)
 2. C. Yoon, et al. arXiv 2005.14710 (2020)
 3. H. G. von Schnerring, et al
Z. Inorg. Chem. 438, **37** (1978).
- H. von Benda, et al.
Z. Inorg. Chem. 438, **53** (1978).

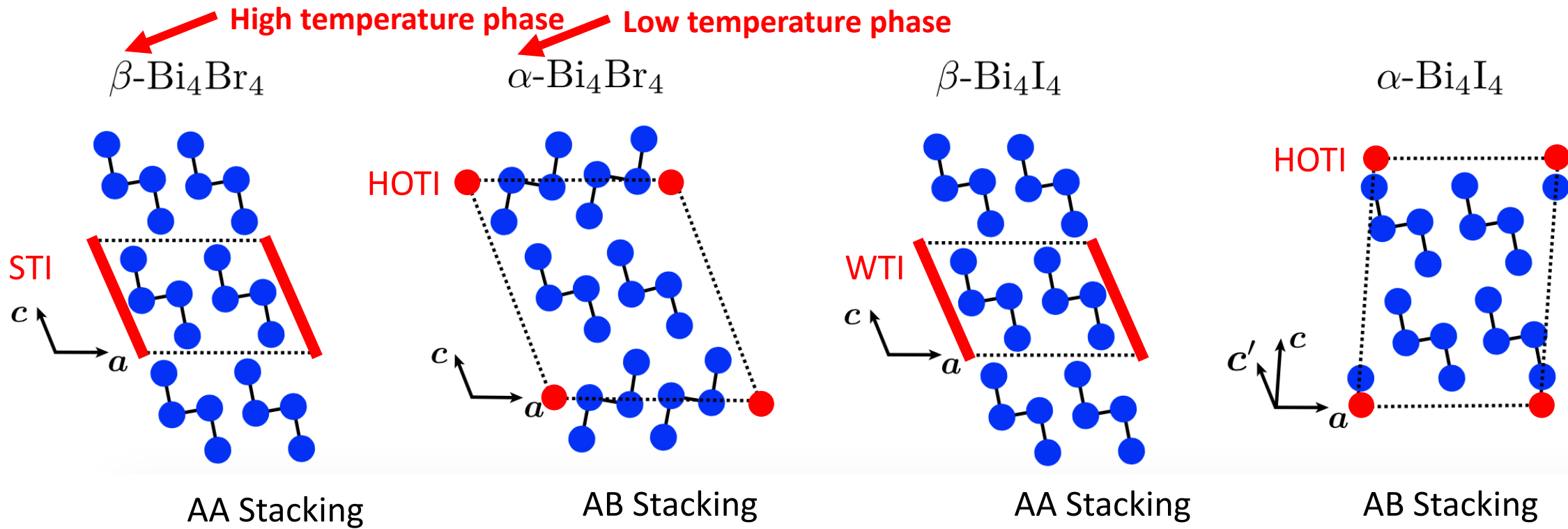


Image courtesy of Bing Lv



Phases of Bismuth Halides

5/27

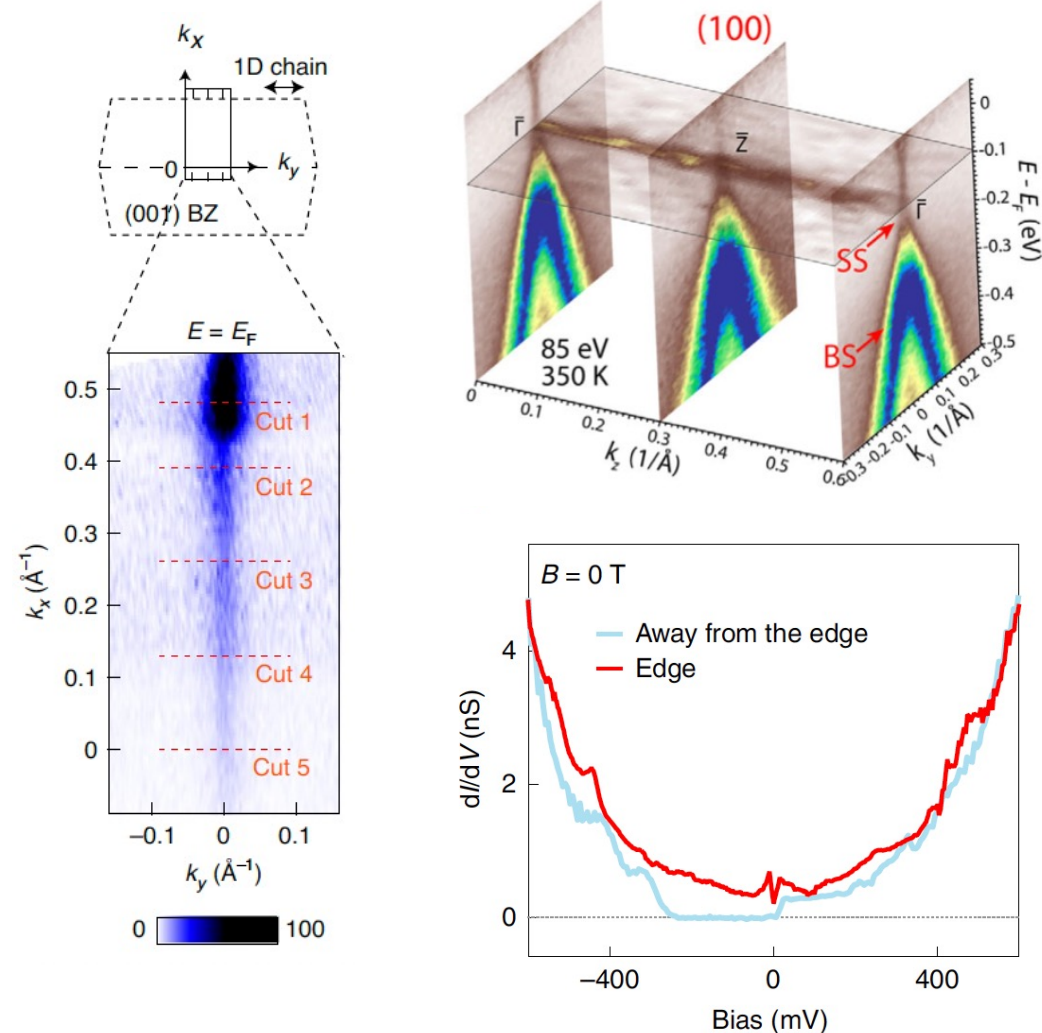


1. C.C. Liu, et al. PRL **116**, 066801 (2016)
2. C. Yoon, et al. arXiv 2005.14710 (2020)
3. R. Noguchi, et al. Nature **566**, 518 (2019)

STM and ARPES Measurements

6/27

- Conclusive evidence for weak TI on (100) surface^{1,2}
- STM evidence of a QSH state on edges³
- Supporting evidence for HOTI on edges⁴
 - Limited by spatial resolution of ARPES



1. R. Noguchi, et al. Nature **566**, 518 (2019)
2. J. Huang, et al. PRX **11**, 031042 (2021)
3. N. Shumiya, et al. Nat. Mater. **21**, 1111 (2022)
4. R. Noguchi, et al. Nat. Mater. **20**, 473 (2021)

Transport Measurements

7/27

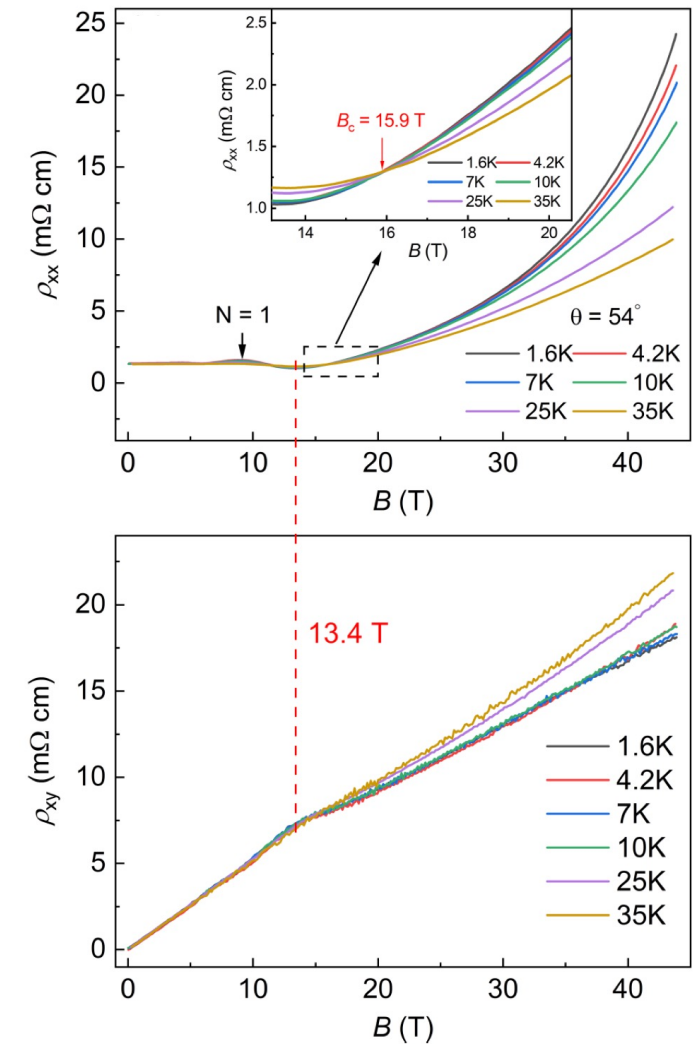
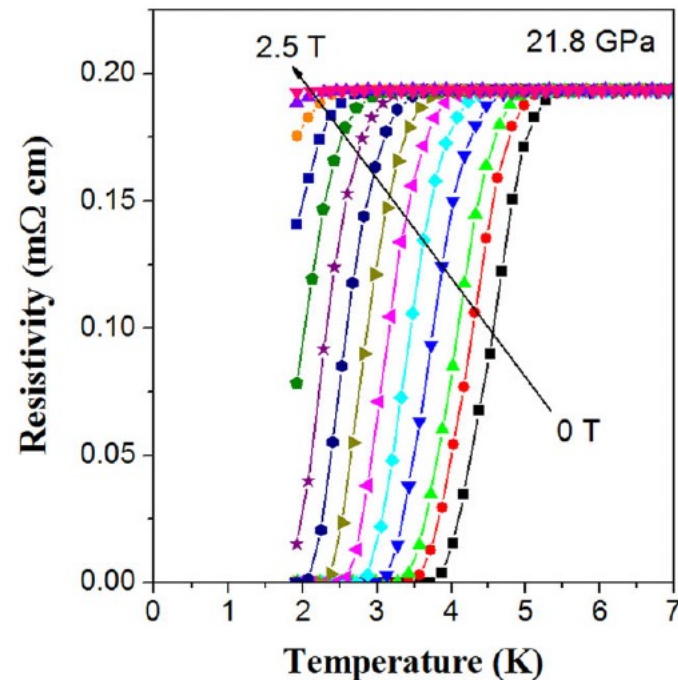
- Pressure induced superconductivity^{1,2}
- Field-induced metal-insulator transition^{3,4}

1. X. Wang, et al. Phys. Rev. B **98**, 174112 (2017)

2. Y. Qi, et al. Npj Q. Mater. 3, 1 (2018)

3. D. Y. Chen, et al. Phys. Rev. Mater. **2**, 114408 (2018)

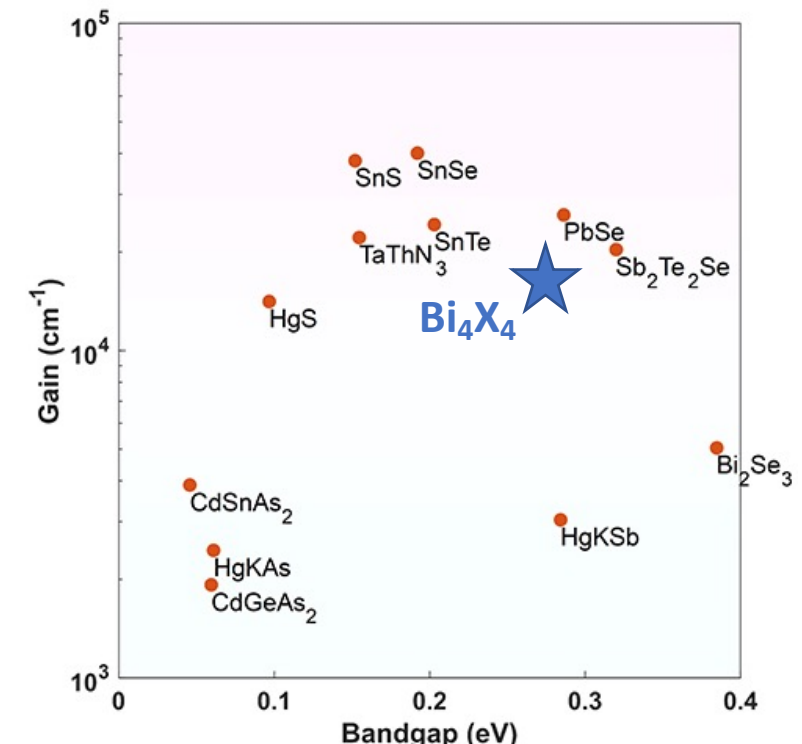
4. P. Wang, et al. Phys. Rev. B **103**, 155201 (2021)



Why Optics?

8/27

- Optical responses can both characterize materials and be used to create devices
 - 1. Anisotropic and “giant” bulk response¹
 - $10^4/\text{cm}$ at the band edge
 - 2. Signatures for surface and edge states
 - Elliptic Dirac cone
 - 3. Quasi-1D surface plasmon polaritons



1. H. Xu, et al. Phys. Chem. Lett. **11**, 6119 (2020)

- Introduction ✓
- Model and methods
- Bulk and (100) side surface optics
- Surface plasmon polaritons
- Conclusion

Our group's
previous work in:
C. Yoon, et al. arXiv
2005.14710 (2020)

The current work



Structure

↓ First-principles DFT

MLWF tight-binding model

↓ Best-fit nearest-neighbor tight-binding model

Hamiltonians and velocity operators

↓ Integrate Kubo formula

Optical conductivity

↓ Textbook formulas

Optical response properties

- Construct layer Hamiltonians
 - All nearest-neighbor hopping terms that preserve inversion symmetry

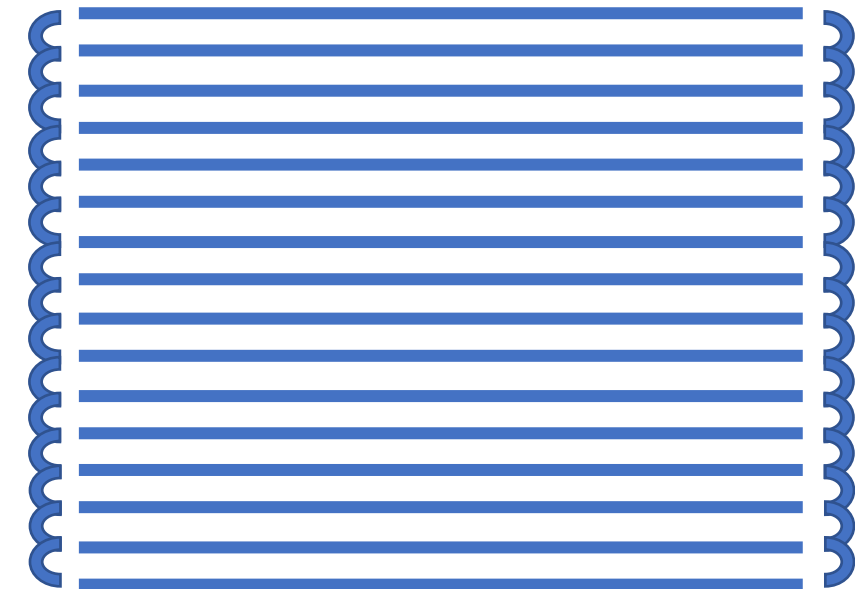
$$H_L = M\sigma_z + D + t_a\sigma_y(\sin(q_1) + \sin(q_2)) + t_b\sigma_x s_z \sin(q_2 - q_1)$$

$$M = m_0 + m_a(\cos(q_1) + \cos(q_2)) + m_b \cos(q_2 - q_1)$$

$$D = d_0 + d_a(\cos(q_1) + \cos(q_2)) + d_b \cos(q_2 - q_1)$$

- Construct bulk Hamiltonians
 - Add inter-layer transfer terms that respect inversion symmetry

$$H_\beta = H_L + 2(d_c + m_c\sigma_z) \cos(q_3) + 2t_c\sigma_x s_y \sin(q_3)$$



1. C. Yoon, et al. arXiv 2005.14710 (2020)

- Dimerizes
- SSH-like model

$$H_6^+ = \begin{pmatrix} H^+ & T_I^- & 0 & 0 & 0 & 0 \\ T_I^+ & H^- & T_E^- & 0 & 0 & 0 \\ 0 & T_E^+ & H^+ & T_I^- & 0 & 0 \\ 0 & 0 & T_I^+ & H^- & T_E^- & 0 \\ 0 & 0 & 0 & T_E^+ & H^+ & T_I^- \\ 0 & 0 & 0 & 0 & T_I^+ & H^- \end{pmatrix}$$

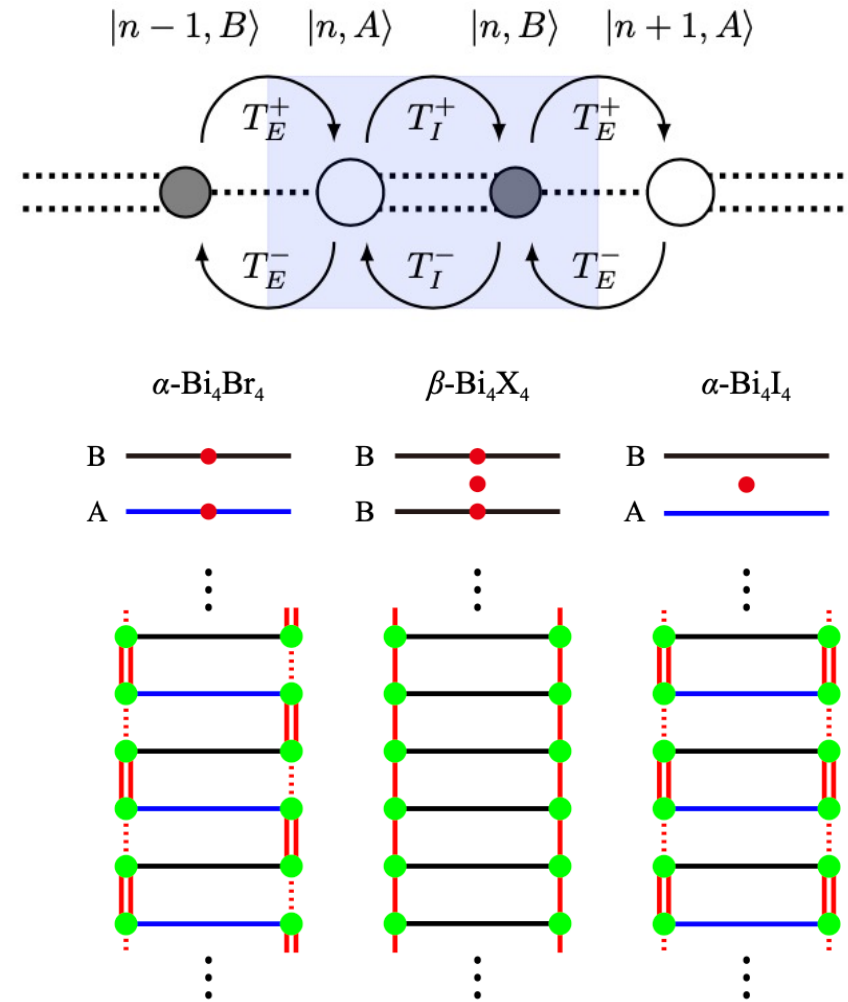
- Layers

$$H^\pm = H_L \pm (t\sigma_x + t'\sigma_y s_y)$$

- Hoppings

$$T_I^\pm = (d_c + m_c \sigma_z) \pm i(\sigma_x s_y t_c)$$

$$T_E^\pm = (d'_c + m'_c \sigma_z) \pm i(\sigma_x s_y t'_c)$$



Model: Edges and Side Surfaces

13/27

- Impose topological boundary conditions on the bulk^{1,2}

$$h_{\beta\text{-I}} = h_E + 2d_c \mathbf{1} + 2\xi t_c s_y q_c$$

$$\begin{aligned} h_{\alpha\text{-I}} = h_E &+ \xi t \tau_z + (d_c \tau_x + d'_c (\tau_x \cos(q_c) + \tau_y \sin(q_c))) \\ &+ \xi s_y (t_c \tau_y - t'_c (\tau_y \cos(q_c) - \tau_x \sin(q_c))) \end{aligned}$$

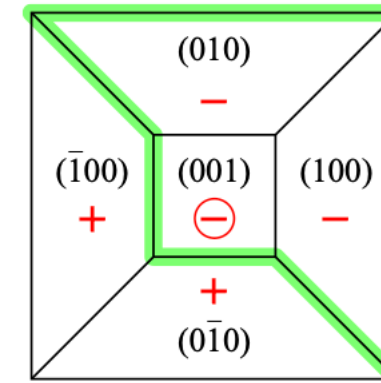
- Edge Hamiltonian

- Consistent with surface and bulk
- Onsite and hopping terms

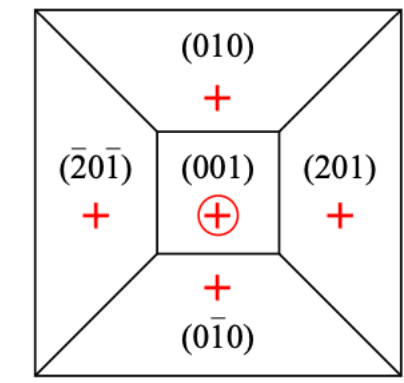
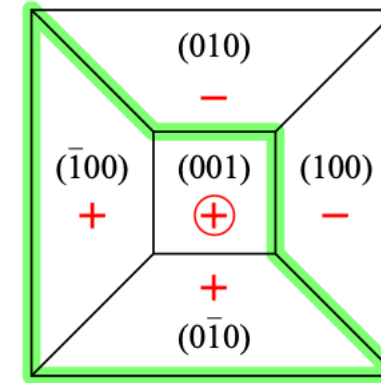
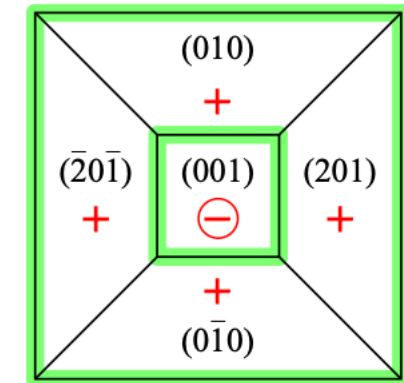
$$h_E = (d_0 - 2d_a + d_b) \mathbf{1} + \xi t_b s_z q_b$$

- F. Zhang, et al. PRL **110**, 046404 (2013)
- C. Yoon, et al. arXiv 2005.14710 (2020)

$\alpha\text{-Bi}_4\text{Br}_4$



$\alpha\text{-Bi}_4\text{I}_4$



- Kubo formula

$$\sigma_{\mu\nu} = i \frac{e^2}{\hbar} \sum_{s, s'} \int_{\text{BZ}} \frac{d\mathbf{k}}{(2\pi)^{\text{dim}}} \frac{1}{\epsilon_{s'} - \epsilon_s} \frac{\langle s, \mathbf{k} | \hbar \frac{\partial \mathcal{H}}{\partial k_\mu} | s', \mathbf{k} \rangle \langle s', \mathbf{k} | \hbar \frac{\partial \mathcal{H}}{\partial k_\nu} | s, \mathbf{k} \rangle}{\hbar\omega - (\epsilon_{s'} - \epsilon_s) + i\eta}$$

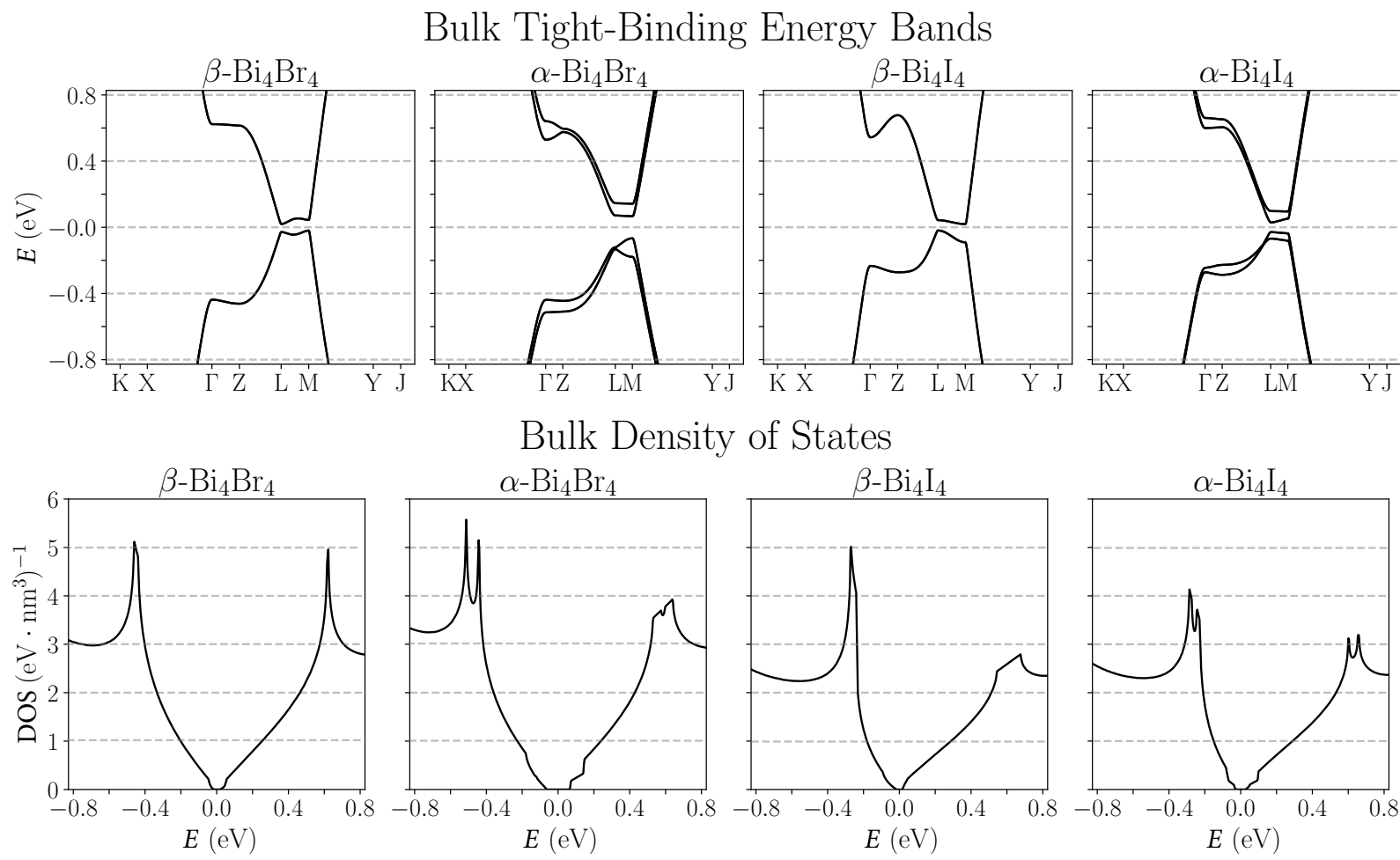
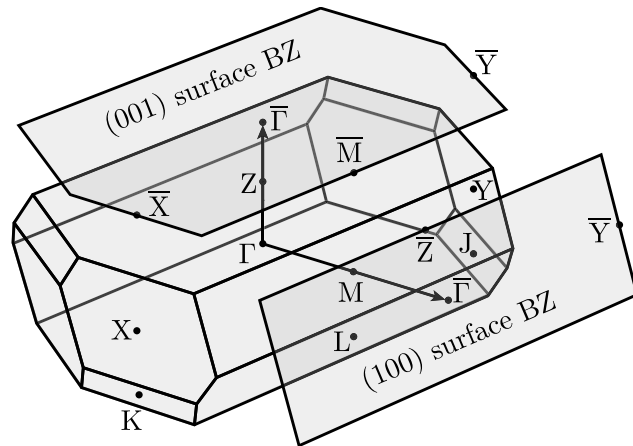
- Numerically integrate

- Low temperature, low scattering rate limit
 - Need many points 10^8 - 10^9 points to converge
- Only some regions of the Brillouin zone are relevant (the Z to M line)
- Method
 - Uniformly sample Brillouin zone
 - Recursively refine over regions with energy conserving transitions

Bulk Band Structures

15/27

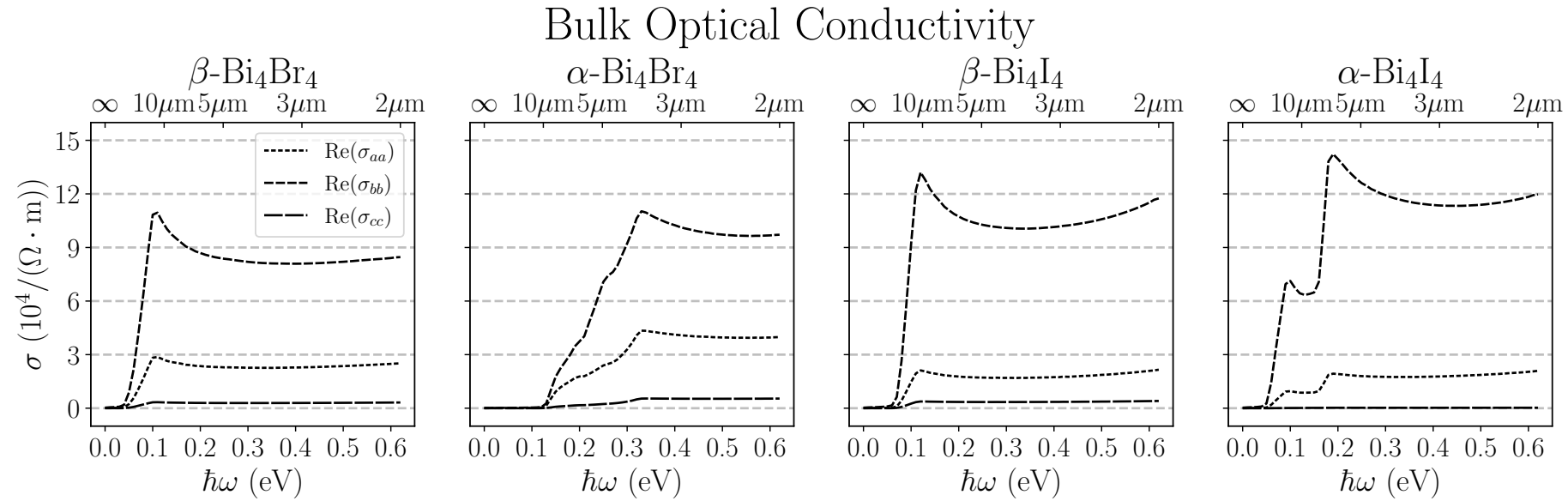
- Bi_4X_4 are bulk insulators
- The energy scale is the IR
- Low-energy physics is on the Gamma-Z-M plane
 - Suggests there will be anisotropic optics



Anisotropic Bulk Response

16/27

- Strand direction conductivity dominates over other directions
- Optical conductivity above the band edge is large
- Absorption is about $10^4/\text{cm}$



Comparison to Experiment

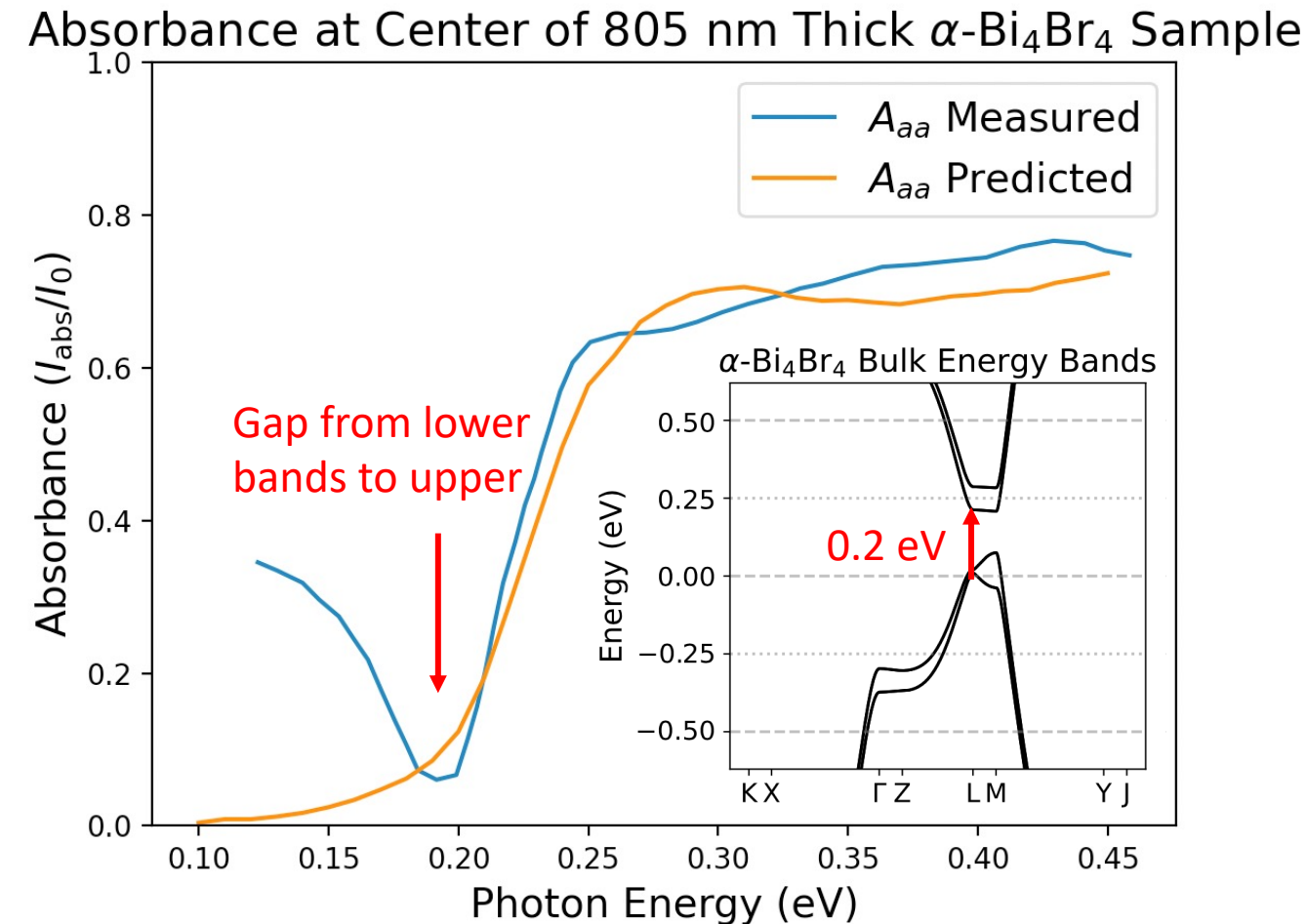
17/27

- **Experiment**

- Crystals grown on CaF_2 substrate by flux method
- Linearly polarized light shined on exposed (001) surface
- Measured absorbance

- **Model**

- Fermi energy 137 meV below center of the bulk band gap
- Beer-Lambert Law
 - $A = (1 - R)(1 - e^{-l \mathcal{A}})$

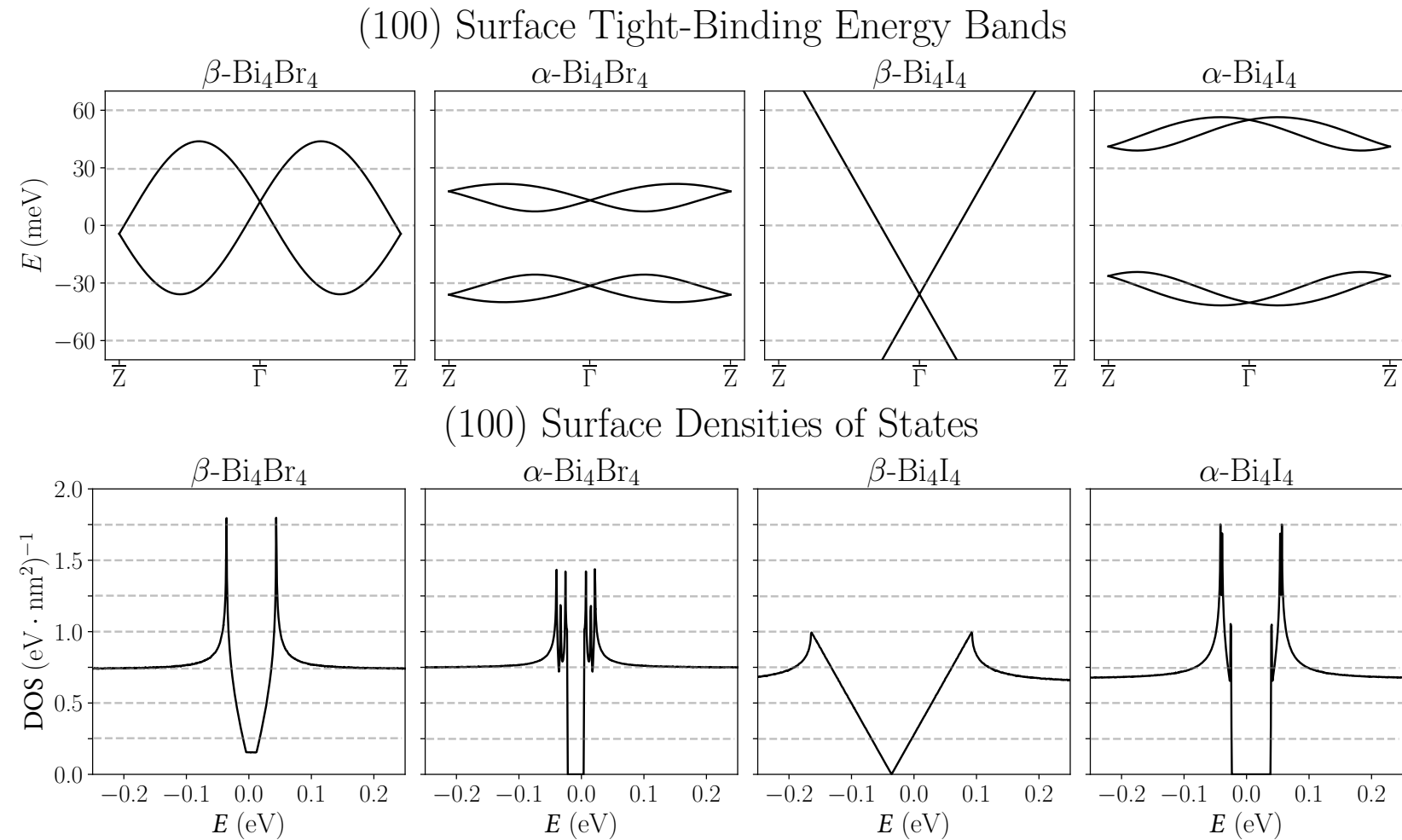


Experimental data from P. Mao, et al. arXiv:2007.00223 (2020).

(100) Surface Band Structure

18/27

- Low energy physics happens around $q_b=0$ since $v_F^b \gg v_F^c$
- Two Dirac cones at different energies (one in STI $\beta\text{-Bi}_4\text{I}_4$)
- $\alpha\text{-Bi}_4\text{Br}_4$ exhibits multiple van Hove singularities versus the other structures which only exhibit two



- Universal optical conductance of 2D Dirac Fermions

$$\sigma = \frac{e^2}{4\hbar}$$

- For elliptic Dirac cones this becomes (quick to derive)

$$\sigma_{\mu\mu} = \frac{(v_F^\mu)^2}{v_F^x v_F^y} \frac{e^2}{4\hbar}$$

- For (100) surface states we have $v_F^b \gg v_F^c$
- Very large (small) and anisotropic response

Optical Absorption of Graphene in the Elliptic Dirac Cone Limit

Let the incident energy flux be (in Gaussian units):

$$W_{\text{incident}} = \frac{\omega^2}{4\pi c} |A|^2 \quad (1.1)$$

And the absorbed power be:

$$W_{\text{absorbed}} = \langle w \rangle \hbar \omega \quad (1.2)$$

Where Fermi's Golden rule gives the transition rate at low temperature ($E_f = \hbar\omega/2$ is the final energy):

$$w = \frac{2\pi}{\hbar} |\langle f | H' | i \rangle|^2 D(E_f) \quad (1.3)$$

Now for graphene in the elliptic Dirac-Cone limit with $\theta = \arg(v_x k_x + iv_y k_y)$:

$$H_0 = \hbar(v_x k_x \sigma_x + v_y k_y \sigma_y) \quad (1.4)$$

$$= \hbar \begin{pmatrix} 0 & v_x k_x - iv_y k_y \\ v_x k_x + iv_y k_y & 0 \end{pmatrix} \quad (1.5)$$

$$= \hbar \sqrt{(v_x k_x)^2 + (v_y k_y)^2} \begin{pmatrix} 0 & e^{-i\theta} \\ e^{i\theta} & 0 \end{pmatrix} \quad (1.6)$$

As above, we consider the perturbations:

$$H'_x = -\frac{e|A|}{\hbar c} \frac{\partial H_0}{\partial k_x} = -\frac{ev_x|A|}{c} \sigma_x \quad (1.7)$$

$$H'_y = -\frac{e|A|}{\hbar c} \frac{\partial H_0}{\partial k_y} = -\frac{ev_y|A|}{c} \sigma_y \quad (1.8)$$

So Fermi's Golden rule gives (for both dir = x, y):

$$w_{\text{dir}} = \frac{2\pi}{\hbar} \left(\frac{ev_{\text{dir}}|A|}{c} \right)^2 \frac{2\sin^2(\theta) + 2\cos^2(\theta)}{4} D(E_f) = \frac{\pi}{\hbar} \left(\frac{ev_{\text{dir}}|A|}{c} \right)^2 D(E_f) = \langle w_{\text{dir}} \rangle \quad (1.9)$$

The number of states per volume is (with $E = \hbar\sqrt{(v_x k_x)^2 + (v_y k_y)^2}$ (recall the area of ellipse is $\pi r_1 r_2$):

$$\frac{N}{V} = \frac{\pi k_x^{\max} k_y^{\max}}{(2\pi)^2} = \frac{\pi E^2}{(2\pi)^2 \hbar v_x v_y} \quad (1.10)$$

So the density of states is (with $E_f = \hbar\omega/2$):

$$D(E_f) = \frac{\hbar\omega}{4\pi\hbar^2 v_x v_y} \quad (1.11)$$

So, we see that the absorption is:

$$P_{\text{dir}}(\omega) = \frac{\langle w \rangle \hbar \omega}{W_{\text{incident}}} \quad (1.12)$$

$$= \hbar \omega \frac{\pi}{\hbar} \left(\frac{ev_{\text{dir}}|A|}{c} \right)^2 \frac{\hbar\omega}{4\pi\hbar^2 v_x v_y} \frac{4\pi c}{\omega^2 |A|^2} \quad (1.13)$$

$$= \frac{\pi e^2}{\hbar c} \frac{v_{\text{dir}}^2}{v_x v_y} \quad (1.14)$$

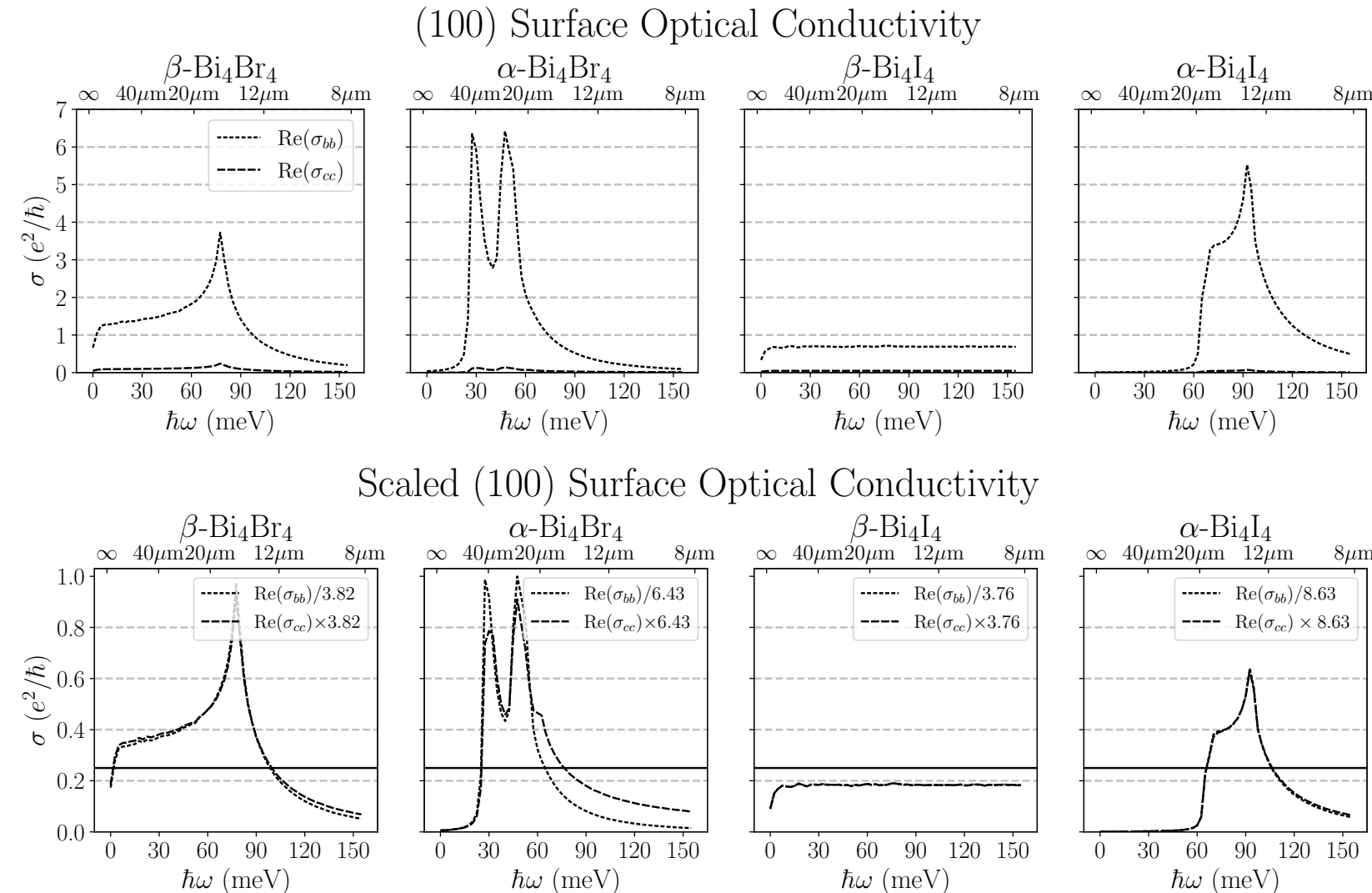
$$= \pi \alpha \frac{v_{\text{dir}}^2}{v_x v_y} \quad (1.15)$$

Which is $\pi\alpha$ when $v_x = v_y$.

Anisotropic (100) Surface Response

20/27

- Optical conductivities are qualitatively like the Dirac conductivity of graphene
 - Except $\alpha\text{-Bi}_4\text{Br}_4$
 - Different JDOS
- Strand direction conductivity dominates transverse conductivity
- Directions are almost related by a scalar multiple (elliptic Dirac)

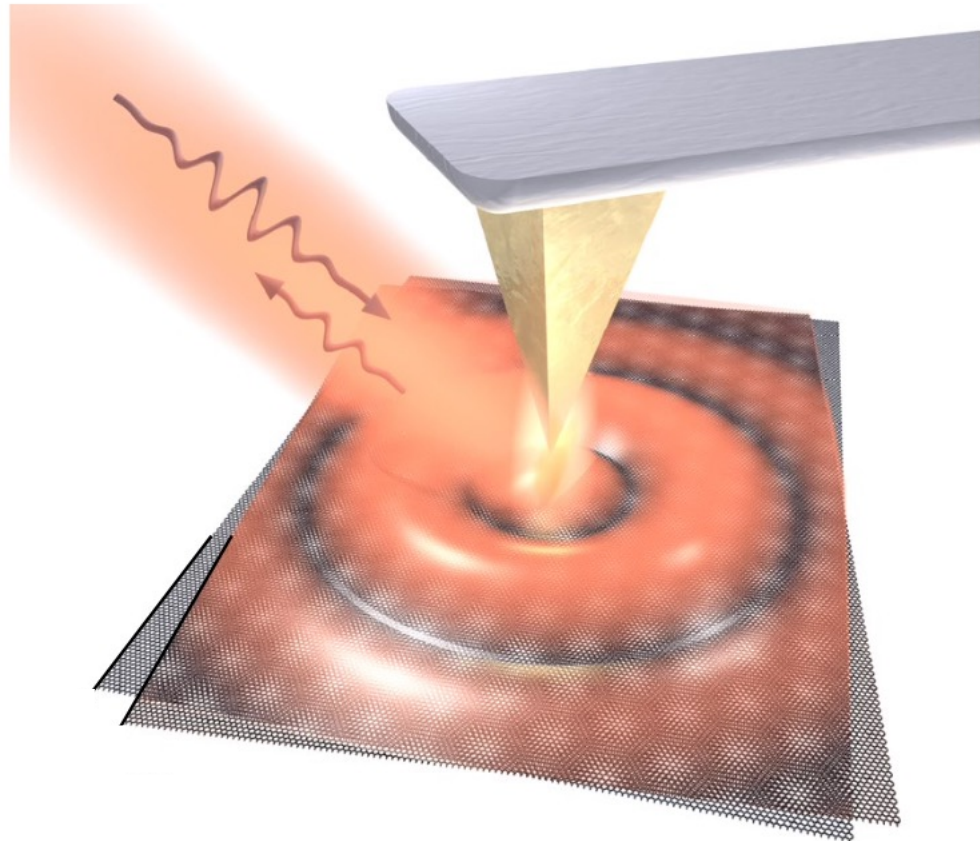


Surface Plasmon Polaritons (SPPs)

21/27

- Plasmon polaritons are near-field quasiparticles that form in materials with negative permittivities
- 3D plasmons are forbidden in Bi_4X_4 since the imaginary part of the optical conductivity is never positive, so the real part of the permittivity is never negative
- Plasmons are described by a quality factor

$$Q_P = \frac{\text{Im}(\sigma)}{\text{Re}(\sigma)}$$



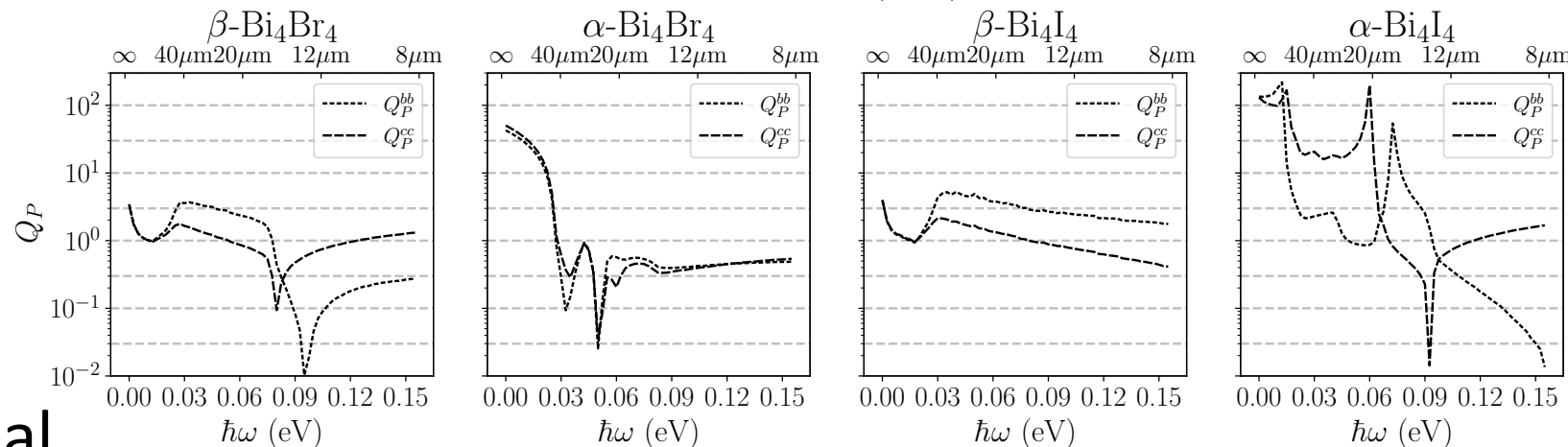
1. N. Hesp, et al. Nat. Phys. **17**, 1161 (2021)

Anisotropic SPPs from (100) Surface States

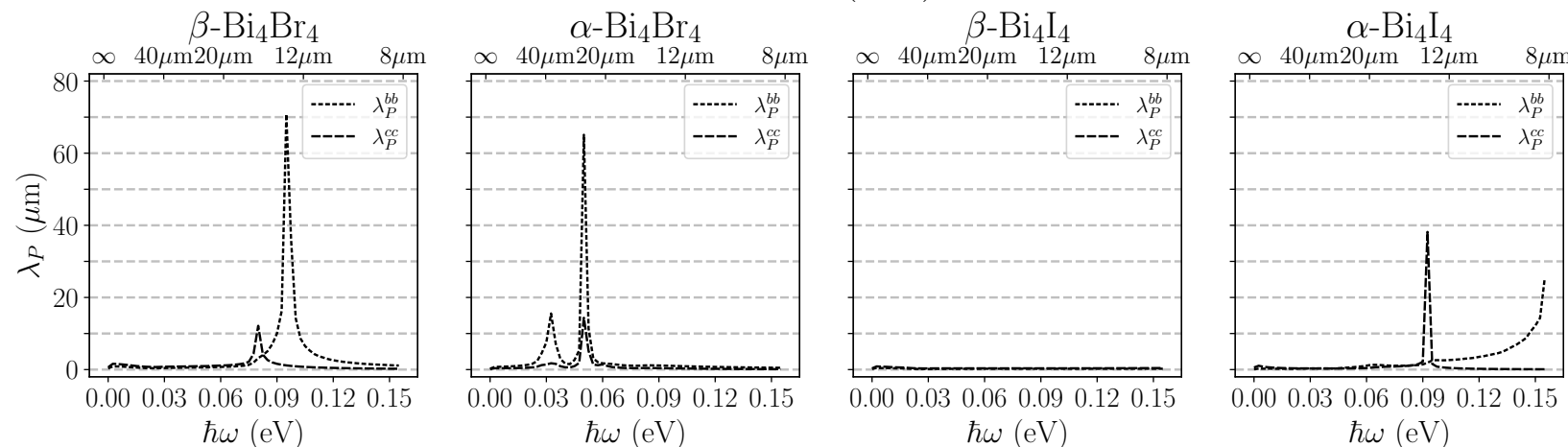
22/27

- Q_P for plasmons in the strand direction and the perpendicular direction can be very different, corresponding to the anisotropy of the material
- This may lead to the formation of quasi-1D SPPs that decay more quickly in one direction than the other

Plasmon Quality Factor for (100) Surface States



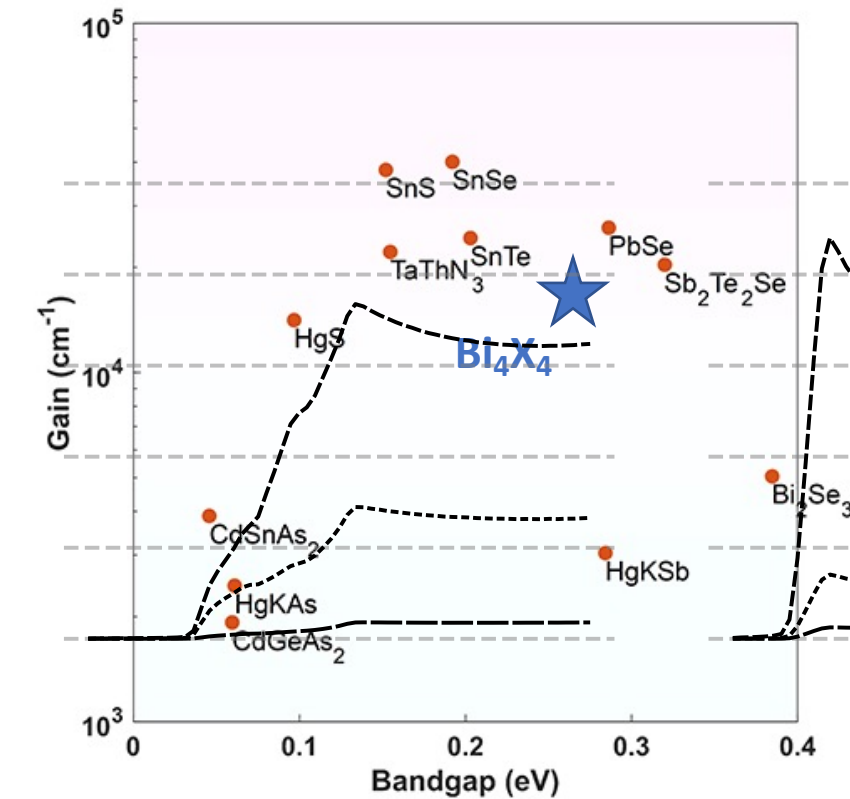
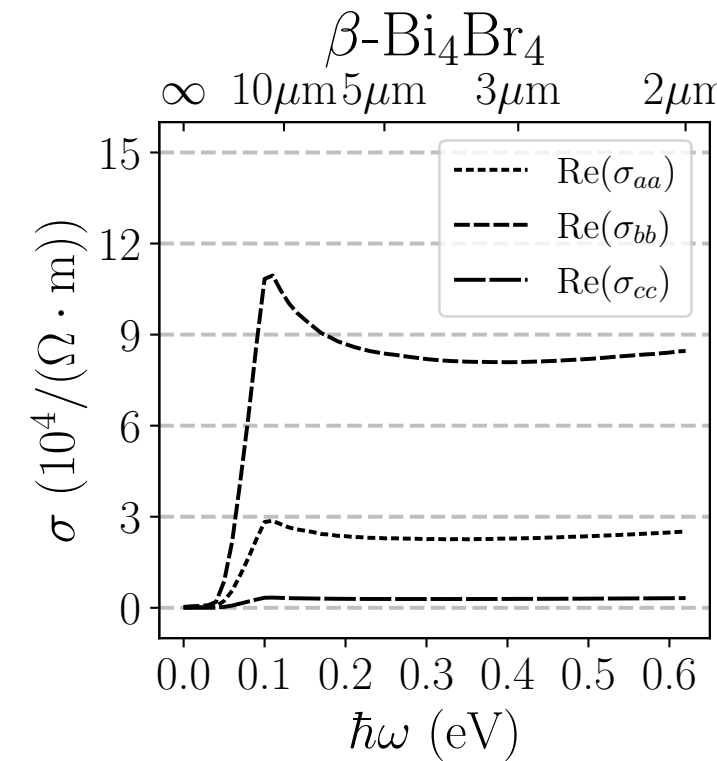
Plasmon Wavelength for (100) Surface States



Result 1: Large and Anisotropic Bulk Response

23/27

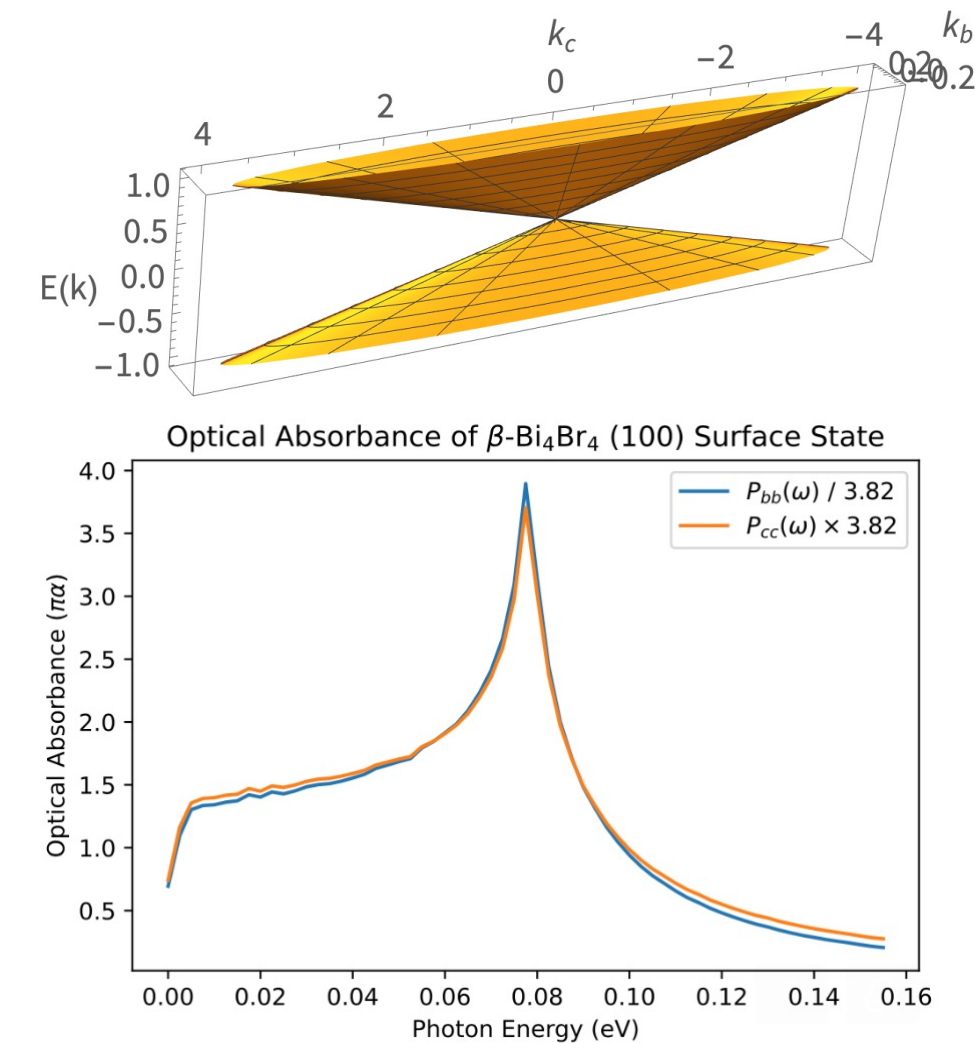
- Optical conductivity and gain surpass conventional HgCdTe photodiodes by an order of magnitude
- Compared to other materials with similar band inversions the response is anisotropic
 - Speculative possibility for polarization-dependent charge coupled photodiodes



Result 2: Signatures of Elliptic Dirac Cones

24/27

- Side surfaces are TIs with one (strong) or two (weak) Dirac cones
- This leads to characteristic conductance and absorbance features
- These materials are quasi-1D
- Conductance features are anisotropic
 - Enhanced in strand direction
 - Suppressed perpendicular to it



Result 3: Quasi-1D Surface Plasmon Polaritons

25/27

- SPPs have been proposed as a platform for room-temperature quantum emitters¹
- Speculatively, quasi-1D SPPs on the (100) surfaces of Bi_4X_4 may provide an avenue for highly polarized quantum emitters²

1. T. Hoang, et al. *Nano. Lett.* **16**, 270 (2016)

2. Q. Wang, et al. *Nano. Lett.* **21**, 7175 (2020)

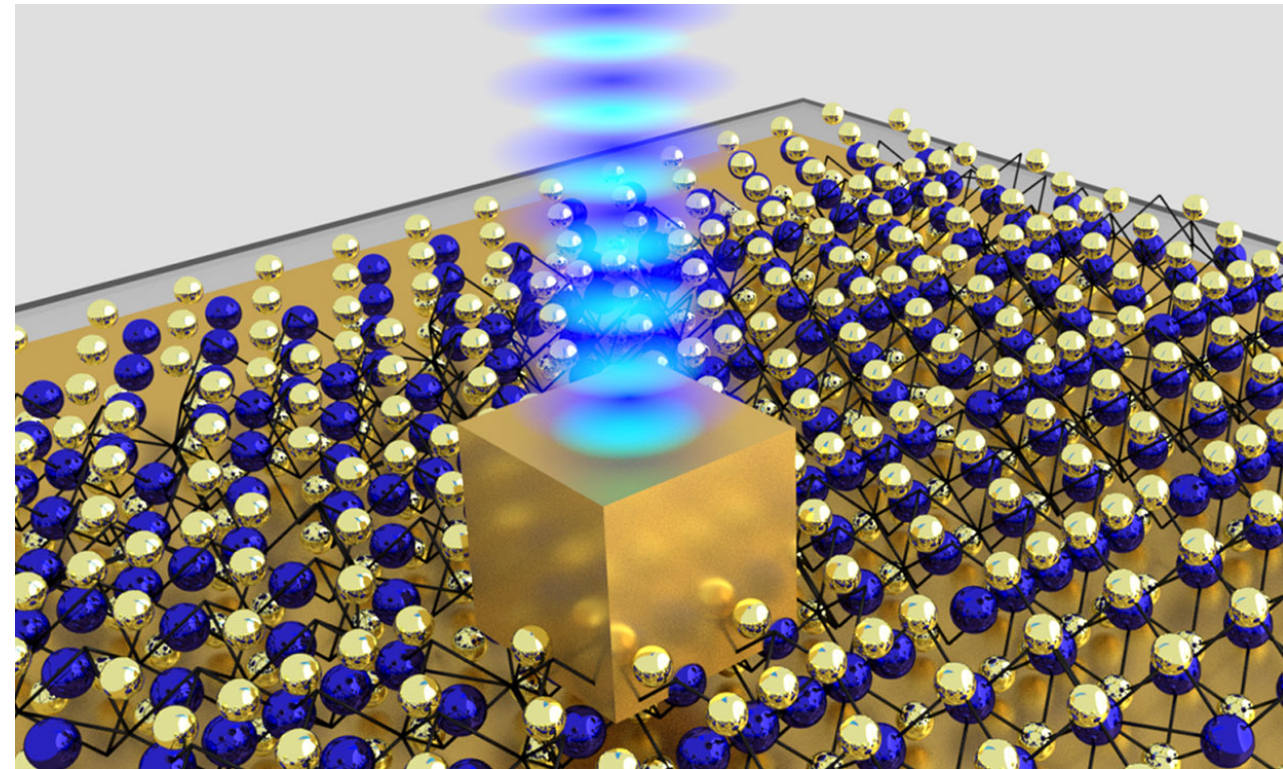


[Image from IEEE Spectrum](#)

- Quasi-1D materials, as exemplified by Bi_4X_4 exhibit a rich and unusual set of electronic states and properties
- Real space, momentum space, and transport studies of these materials have elucidated the properties of these materials
- A speculative frontier for Bi_4X_4 in optoelectronics
 - Polarized large gain charge coupled diodes
 - Polarized quantum emitters

Acknowledgements

27/27

S.T. and F.Z. acknowledge support from the NSF under DMREF Grant No. DMR-1921581, and from the Army Research Office under Grant No. W911NF-18-1-0416.

S.T. acknowledges support from the NSF under Grant No. DGE-1845298, the NSF under Grant No. PHY-1757503, and the Barry Goldwater Foundation.

